
Graph Generation via Spectral Diffusion

Giorgia Minello¹ Alessandro Biciato¹ Luca Rossi² Andrea Torsello¹ Luca Cosmo¹

Abstract

In this paper, we present GRASP, a novel graph generative model based on 1) the spectral decomposition of the graph Laplacian matrix and 2) a diffusion process. Specifically, we propose to use a denoising model to sample eigenvectors and eigenvalues from which we can reconstruct the graph Laplacian and adjacency matrix. Our permutation invariant model can also handle node features by concatenating them to the eigenvectors of each node. Using the Laplacian spectrum allows us to naturally capture the structural characteristics of the graph and work directly in the node space while avoiding the quadratic complexity bottleneck that limits the applicability of other methods. This is achieved by truncating the spectrum, which as we show in our experiments results in a faster yet accurate generative process. An extensive set of experiments on both synthetic and real world graphs demonstrates the strengths of our model against state-of-the-art alternatives.

1. Introduction

Generating realistic graphs by learning from a distribution of real-world graphs has gained increasing attention from researchers in many fields, due to its wide range of applications. For instance, synthetic graph generation plays a crucial role in drug design (Gómez-Bombarelli et al., 2018; Li et al., 2018b; You et al., 2018a) as well as in network science (Watts & Strogatz, 1998; Leskovec et al., 2010; Albert & Barabási, 2002).

Traditional graph generation approaches date back to the 1960s and rely on simple stochastic processes, limiting their ability to capture complex dependencies seen in real-world networks. For example, the Barabási-Albert (Albert & Barabási, 2002) and Kronecker (Leskovec et al., 2010) graph models are specifically designed to generate graphs belonging to specific families and lack the ability to learn

directly from observed data. While these models may excel in capturing a set of predefined properties, they are often unable to represent a wider range of aspects observed in real-world graphs. In addition, in several domains network properties are largely unknown, which further limits the applicability of these traditional techniques. For instance, the Barabási-Albert model (Albert & Barabási, 2002) allows to create graphs that exhibit the scale-free nature found in empirical degree distributions, however it is unable to capture other facets of real-world graphs, *e.g.*, community structure. Overcoming these shortcomings has then become a necessary step towards enhancing the expressivity and fidelity of generated graphs, which in turn would extend the range of possible applications of graph generative models.

In this paper we introduce a new model for GRAPh generation via SPectral diffusion (GRASP)¹. The ideas underpinning our approach are 1) to represent the graph using the eigendecomposition of its Laplacian matrix and 2) to use a diffusion-based approach to learn to sample sets of eigenvalues and eigenvectors from which a graph adjacency matrix can be reconstructed. Doing this allows us to work directly in the space of nodes while overcoming the computational bottleneck (quadratic in the number of graph nodes) of other methods that follow a similar approach (Vignac et al., 2022). Unlike other closely related models (Martinkus et al., 2022), GRASP is able to directly generate eigenvalues and eigenvectors, instead of interpolating them from ground truth data (Martinkus et al., 2022), and it can naturally handle both discrete and continuous node features. Working in the spectral domain is crucial to overcoming the computational bottleneck, as it allows us to limit the number of eigenvalues and eigenvectors used to reconstruct the graph adjacency matrix, while at the same time encapsulating graph structural characteristics. Our model also allows us to condition the generation of new graphs on desired spectral properties.

The remainder of this paper is structured as follows. Section 2 reviews the related work, while Sections 3 and 4 introduce the necessary background on denoising diffusion models and spectral graph theory, respectively. We introduce our graph generative model in Section 5 and we present the experimental evaluation against state-of-the-art alternatives in Section 6. Finally, Section 7 concludes the paper.

¹Ca' Foscari University of Venice, Italy ²The Hong Kong Polytechnic University, Hong Kong. Correspondence to: Luca Rossi <luca.rossi@polyu.edu.hk>.

¹<https://github.com/lcosmo/GRASP>.

2. Related Work

In contrast to the image and text domains, where the development of generative models is well understood and established, graphs introduce a series of additional challenges.

The first issue is the non-uniqueness of graph representations, *i.e.*, if a graph contains n nodes, there exist up to $n!$ distinct adjacency matrices that serve as equivalent representations of the same graph. Ideally, a generative model should assign equal probability to each of these $n!$ adjacency matrices. Another crux lies in the size of the output space, which is quadratic in the number of nodes and that quickly become a bottleneck when dealing with large graphs. Graph generative models should also be able to take into account the existence of dependencies and relationships between nodes and edges, rather than treating them as independent, *e.g.*, in social networks the likelihood of two nodes being connected is often higher when they have common neighbors. Finally, standard machine learning techniques designed for continuously differentiable objective functions are unsuitable to be directly applied to discrete graph structures (Guo & Zhao, 2022).

Traditional graph generative model approaches seek to address these problems, yet focus only on the generation of graphs displaying a limited set of structural characteristics. These initial methods rely on identifying common characteristics in real-world graphs, such as degree distribution, graph diameter, and clustering coefficient (Faloutsos, 2008), and then generate synthetic graphs through the application of a set of heuristic rules (Leskovec et al., 2010; Leskovec & Faloutsos, 2007; Erdős et al., 1960; Albert & Barabási, 2002). Although these models can produce synthetic graphs with the given desired features, they are limited in their ability to generate node features as well as novel structural patterns.

A breakthrough in this field has been marked by the recent progress in deep learning models such as Variational Auto Encoders (VAEs) (Kingma & Welling, 2013), Recurrent Neural Networks (RNNs) (Zaremba et al., 2014) and Generative Adversarial Networks (GANs) (Goodfellow et al., 2014). In this context, we encounter models commonly referred to as *general-purpose deep graph generative models*, such as GraphRNN (You et al., 2018b) and GRAN (Liao et al., 2019), which exploit deep architectures to learn the graphs distribution. Even though they represent a step forward in the field of generative graph models, most of them are limited by exclusively focusing on the graph structure. Further, approaches of this type adopt evaluation metrics based only on graph statistics, like degree distribution or clustering coefficients, and thus overlook or omit the assessment of the generated node features.

Node and edge features are instead considered in a num-

ber of methods developed specifically for the generation of molecules, indeed one of the most promising application scenario for modern graph generation approaches. Models falling in this domain, referred to as *molecule graph generative models*, exploit deep architectures such as GAN in (De Cao & Kipf, 2018) or RNN in (Popova et al., 2019) as well as other generation strategies (*e.g.*, graph normalizing flows (Luo et al., 2021)) or the combination of different approaches. For instance, (Shi et al., 2020) combines the advantages of both autoregressive and flow-based methods.

Nevertheless, there are other deep learning approaches beyond molecule graph generative models that are capable of generating graphs with node and edge features - even though the evaluation itself is often still based on a molecule generation task. For instance (Simonovsky & Komodakis, 2018) and (Grover et al., 2019) propose general deep generative models for graphs based on variational autoencoders. The main drawback of these architectures is that they are specialized and limited to small-scale graphs with low-dimensional feature space (Yoon et al., 2023).

Another category of graph generative models takes cues from the score-based generative modeling work of Song & Ermon to define diffusion models for graphs. For instance, in (Huang et al., 2022) the authors propose a forward diffusion process, specifically a continuous-time generative diffusion process for permutation invariant graph generation. Similarly, (Niu et al., 2020) introduce a different diffusion model named Edge-wise Dense Prediction Graph Neural Network (EDP-GNN), which uses Gaussian noise and uses thresholding to address the issue of generating a discrete valued adjacency matrix from continuous values. Crucially, the proposed method cannot fully capture node-edge dependencies. A similar score-based generative model for graphs, where both node features and adjacency matrix are created, is presented in (Jo et al., 2022). Finally, (Vignac et al., 2022) suggest an alternative approach where a discrete diffusion process is used to generate graphs with discrete node and edge features. This is similar to (Haefeli et al., 2022), however the latter can only be applied to unattributed graphs.

More recently, (Martinkus et al., 2022) with their SPECTRE network and (Luo et al., 2023) take a different approach by considering the graph spectra, thus leveraging the inherent ability of the low frequency portion of the spectrum to capture global structural characteristics of the corresponding graph. While closely related to our method, it should be noted that SPECTRE does not directly generate the eigenvectors as GRASP does, rather it uses ground truth data to interpolate them. DiGress (Vignac et al., 2022) is also closely related to our model, however its complexity is quadratic in the number of nodes of the graph, making it unsuitable to work on large graphs.

3. Denoising Diffusion Models

Denoising Diffusion Probabilistic Models (DDPMs) are a class of generative models inspired by considerations from non-equilibrium thermodynamics. In particular, diffusion models in deep learning were first introduced in (Sohl-Dickstein et al., 2015) yet popularized only in 2020 (Ho et al., 2020). They operate by iteratively introducing noise to an input signal and then learning to denoise by generating new samples from the corrupted signals.

Specifically, the idea is to destroy the structure in a data distribution through an iterative forward diffusion process (noising) and then learn a reverse diffusion process (denoising). This reverse process restores structure in the data, thus yielding a tractable generative model of the data.

Given a data point sampled from a real but unknown data distribution $\mathbf{x}_0 \sim q(\mathbf{x})$, we define a forward noising process q producing a sequence of noisy samples $\mathbf{x}_1, \dots, \mathbf{x}_T$ as a Markov Chain given by

$$q(\mathbf{x}_1, \dots, \mathbf{x}_T | \mathbf{x}_0) = \prod_{t=1}^T q(\mathbf{x}_t | \mathbf{x}_{t-1}), \quad (1)$$

where

$$q(\mathbf{x}_t | \mathbf{x}_{t-1}) = \mathcal{N}(\mathbf{x}_t; \sqrt{1 - \beta_t} \mathbf{x}_{t-1}, \beta_t \mathbf{I}), \quad (2)$$

is the forward diffusion kernel.

Eq. 2 can be reformulated as a single step, *i.e.*,

$$q(\mathbf{x}_t | \mathbf{x}_0) = \mathcal{N}(\mathbf{x}_t; \sqrt{\bar{\alpha}_t} \mathbf{x}_0, (1 - \bar{\alpha}_t) \mathbf{I}), \quad (3)$$

where $\bar{\alpha}_t = \prod_{s=1}^t (1 - \beta_s)$.

The forward diffusion process is fixed and known, *i.e.*, we know the probability density function (PDF) of the data \mathbf{x}_t at time-step t in the forward diffusion process given \mathbf{x}_{t-1} . In particular, the PDF used to define the forward diffusion kernel is a Gaussian distribution. Stated otherwise, this transition function adds at each step a small amount of Gaussian noise to the sample data. The parameters defining the distribution of each sample \mathbf{x}_t are the mean $\sqrt{1 - \beta_t} \mathbf{x}_{t-1}$ and the covariance $\beta_t \mathbf{I}$. Here the term β (the diffusion rate) is pre-calculated by a variance scheduler $\{\beta_t \in (0, 1)\}_{t=1}^T$, *i.e.*, the amount of noise added is regulated by the scheduler. When $T \rightarrow \infty$, \mathbf{x}_T will be nearly equivalent to an isotropic Gaussian distribution. In other words, the schedule of the β_t values (the noise schedule) is designed such that $\bar{\alpha}_T \rightarrow 0$ and $q(\mathbf{x}_T | \mathbf{x}_0) \approx \mathcal{N}(\mathbf{x}_T; 0, \mathbf{I})$.

In the reverse diffusion process, the goal is to recreate the true sample from a Gaussian noise input $\mathbf{x}_T \sim \mathcal{N}(\mathbf{0}, \mathbf{I})$ by sampling from $q(\mathbf{x}_{t-1} | \mathbf{x}_t)$, the true denoising distribution. Notably, if β_t is small in each forward diffusion step, we can use a Gaussian distribution to approximate $q(\mathbf{x}_{t-1} | \mathbf{x}_t)$. In order to run the reverse diffusion process we need to learn a

model p_θ to approximate these conditional probabilities.

As (Feller, 1949) showed, in the case of Gaussian distributions the diffusion process reversal has the same functional form of the forward process. From this it follows that the reverse diffusion process kernel can be defined as

$$p_\theta(\mathbf{x}_{t-1} | \mathbf{x}_t) = \mathcal{N}(\mathbf{x}_{t-1}; \boldsymbol{\mu}_\theta(\mathbf{x}_t, t), \boldsymbol{\Sigma}_\theta(\mathbf{x}_t, t)), \quad (4)$$

where θ are the parameters of the reverse diffusion kernel at each time step, which can be learned using a neural network. If we fix the variance to a constant β_t , we only need to learn the distance between the means of two Gaussian distributions, *i.e.*, between the noise added in the forward process and the noise predicted by the model. This leads to a variational lower bound loss expressed in terms of the Kullback–Leibler (KL) divergence between the posterior of the forward process and the parameterized reverse diffusion process,

$$L_{t-1} = D_{KL}(q(\mathbf{x}_{t-1} | \mathbf{x}_t, \mathbf{x}_0) \| p_\theta(\mathbf{x}_{t-1} | \mathbf{x}_t)). \quad (5)$$

The forward process posterior distribution is

$$q(\mathbf{x}_{t-1} | \mathbf{x}_t, \mathbf{x}_0) = \mathcal{N}(\mathbf{x}_{t-1}; \tilde{\boldsymbol{\mu}}_t(\mathbf{x}_t, \mathbf{x}_0), \tilde{\boldsymbol{\beta}}_t \mathbf{I}), \quad (6)$$

where $\tilde{\boldsymbol{\mu}}_t(\mathbf{x}_t, \mathbf{x}_0) = \frac{\sqrt{\bar{\alpha}_{t-1} \beta_t}}{1 - \bar{\alpha}_t} \mathbf{x}_0 + \frac{\sqrt{\bar{\alpha}_t (1 - \bar{\alpha}_{t-1})}}{1 - \bar{\alpha}_t} \mathbf{x}_t$ and $\tilde{\boldsymbol{\beta}}_t = \frac{1 - \bar{\alpha}_{t-1}}{1 - \bar{\alpha}_t} \beta_t$.

During the training phase the model needs to estimate the parameters of the posterior such that the KL divergence is minimized. This in turn can be accomplished by minimizing the difference between the two means of the Gaussian distributions, *i.e.*,

$$L_{t-1} = \mathbb{E}_q \left[\frac{1}{2\sigma_t^2} \|\tilde{\boldsymbol{\mu}}_t(\mathbf{x}_t, \mathbf{x}_0) - \boldsymbol{\mu}_\theta(\mathbf{x}_t, t)\|^2 \right] + C. \quad (7)$$

In other words, this means predicting the noise at each time step. In order to do this, we reformulate both $\tilde{\boldsymbol{\mu}}$ and $\boldsymbol{\mu}_\theta$ as

$$\tilde{\boldsymbol{\mu}}(\mathbf{x}_t, \mathbf{x}_0) = \frac{1}{\sqrt{\bar{\alpha}_t}} \left(\mathbf{x}_t - \frac{\beta_t}{\sqrt{1 - \bar{\alpha}_t}} \boldsymbol{\epsilon}_t \right) \quad (8)$$

$$\boldsymbol{\mu}_\theta(\mathbf{x}_t, \mathbf{x}_0) = \frac{1}{\sqrt{\bar{\alpha}_t}} \left(\mathbf{x}_t - \frac{\beta_t}{\sqrt{1 - \bar{\alpha}_t}} \boldsymbol{\epsilon}_\theta(\mathbf{x}_t, t) \right) \quad (9)$$

which, after simplification, yields the loss

$$L_{final} = \mathbb{E}_{t, \mathbf{x}_0, \boldsymbol{\epsilon}} [\|\boldsymbol{\epsilon} - \boldsymbol{\epsilon}_\theta(\mathbf{x}_t, t)\|^2]. \quad (10)$$

4. Spectral Graph Theory

Consider an undirected unweighted graph $\mathcal{G} = (\mathcal{V}, \mathcal{E})$, where \mathcal{V} is the set of n nodes connected by the edge set \mathcal{E} . The adjacency matrix of \mathcal{G} is the binary symmetric matrix \mathbf{A} such that $\mathbf{A}_{i,j} = 1$ if the i -th and j -th node are connected by an edge, zero otherwise.

The graph Laplacian of a graph \mathcal{G} with adjacency matrix \mathbf{A} is the positive-semidefinite matrix $\mathbf{L} = \mathbf{D} - \mathbf{A}$, where

\mathbf{D} is the diagonal degree matrix with non-zero elements $\mathbf{D}_{i,i} = \sum_{j=1}^n \mathbf{A}_{i,j}$. The spectrum of the graph Laplacian is $\mathbf{L} = \mathbf{\Phi}\mathbf{\Lambda}\mathbf{\Phi}^\top$, where $\mathbf{\Phi}$ is the orthonormal matrix of eigenvectors (as columns) and $\mathbf{\Lambda} = \text{diag}(\lambda_1, \dots, \lambda_n)$ is the diagonal matrix of eigenvalues, with $0 \leq \lambda_1 \leq \dots \leq \lambda_n$. In the following sections, we denote as $\boldsymbol{\lambda}$ the vector of eigenvalues of the graph Laplacian, *i.e.*, the diagonal of the Laplacian matrix.

The fundamental intuition underpinning our model is that we can represent the graph connectivity with (possibly a subset of) the eigenvectors $\mathbf{\Phi}$ and the corresponding eigenvalues $\boldsymbol{\lambda}$ of the graph Laplacian. The connection between the spectrum of the graph Laplacian and the structural properties of the underlying graph is well known and studied. For example, it is well established that the low frequency portion of the spectrum captures the global structural characteristic of the graph, while the high frequencies are essential in the reconstruction of local connectivity patterns.

5. Spectral Diffusion

Moving from the Laplacian to its spectrum reduces the double row-, column-covariance with respect to node permutations of the Laplacian matrix, to a single covariance over the rows of the eigenvector matrix. To address this covariance, we represent the eigenvector matrix as a series of spectral embedding of the nodes, *i.e.*, we interpret the i -th component of the j -th eigenvector as the j -th component of the i -th node embedding, or alternatively, we see the rows of $\mathbf{\Phi}$ as vectors. To this we add the eigenvalues $\boldsymbol{\lambda}$ as a global graph descriptor. With this representation to hand, we define the diffusion steps as

$$p_\theta(\mathbf{\Phi}_{t-1}, \boldsymbol{\lambda}_{t-1} | \mathbf{\Phi}_t, \boldsymbol{\lambda}_t) = \mathcal{N}(\{\mathbf{\Phi}_{t-1}, \boldsymbol{\lambda}_{t-1}\}; \boldsymbol{\mu}_\theta(\mathbf{\Phi}_t, \boldsymbol{\lambda}_t, t), \sigma_t^2 \mathbf{I}), \quad (11)$$

where the normal distribution is over the product set of the spectral embeddings and the global spectral descriptor.

Fig. 1 shows an overview of the GRASP pipeline. This is made of two main components, namely 1) the spectral diffusion process and 2) the graph predictor, which are discussed in detail in the following subsections.

Following DDPM (Ho et al., 2020), we train a neural network to predict the denoising step. We design the backbone of our spectral diffusion process of Eq. 11 as a neural network composed of a sequence of layers containing a pair of multi-head attention blocks (Vaswani et al., 2017), one operating on the eigenvectors conditioned on the eigenvalues and one operating on the eigenvalues conditioned by the eigenvectors. This choice allows us to achieve both a node permutation invariant model and to let the eigenvectors and eigenvalues condition each other on the prediction of the denoising step. Moreover, this model can easily handle

node features \mathbf{X} by simply concatenating them to the eigenvectors of each node. Fig. 2 shows the overall structure of the proposed neural network.

5.1. Reduced Spectrum and Diffusion Complexity

By fixing the maximum number of eigenvectors to k , we reduce the memory footprint of the diffusion model from $O(n^2)$ to $O(kn)$, where n denotes the number of graph nodes, resulting in a faster generative process.

For this reason, for larger graphs, we perform diffusion on a subset of k eigenvectors. In this case, after the denoising diffusion process, we obtain a subset $\tilde{\mathbf{\Phi}}$ of columns of $\mathbf{\Phi}$ with the corresponding subset of eigenvalues $\tilde{\boldsymbol{\lambda}}$, which allows for an approximated reconstruction of $\tilde{\mathbf{L}} = \tilde{\mathbf{\Phi}}\tilde{\boldsymbol{\lambda}}\tilde{\mathbf{\Phi}} \approx \mathbf{L}$, from which the adjacency matrix can be inferred.

Interestingly, we experimentally observe that eigenvectors associated with larger eigenvalues (higher frequencies) convey more information about the connectivity and allow for better reconstructions of the original adjacency matrix (see subsection B). Note that this is in stark contrast to SPECTRE (Martinkus et al., 2022), where the spectrum is truncated to include only low frequency information.

5.2. Graph Predictor

The main drawback of considering a subset of the eigenvectors is the introduction of noise on the reconstructed adjacency matrix. We adopt a strategy similar to the one proposed in SPECTRE (Martinkus et al., 2022) to predict a binary adjacency matrix starting from a noisy reconstruction. We train a l -layer Provably Powerful Graph Network (PPGN) (Maron et al., 2019), which takes as input the generated eigenvectors $\tilde{\mathbf{\Phi}}$ scaled by the square root of the eigenvalues $\tilde{\boldsymbol{\lambda}}$ as node features as well as the noisy adjacency matrix $\tilde{\mathbf{A}} = \tilde{\mathbf{D}} - \tilde{\mathbf{L}}$ and predicts the binary adjacency matrix

$$\mathcal{A}(\tilde{\mathbf{\Phi}}, \tilde{\boldsymbol{\lambda}}) = \gamma(\text{PPGN}_l(\tilde{\mathbf{A}}, \tilde{\mathbf{\Phi}}\tilde{\boldsymbol{\lambda}}^{\frac{1}{2}})), \quad (12)$$

where γ is a sigmoid activation function and PPGN_l is a sequence of PPGN layers.

We train this network with two losses: 1) a reconstruction loss on the eigenvectors $\tilde{\mathbf{\Phi}}_{gt}$ and eigenvalues $\tilde{\boldsymbol{\lambda}}_{gt}$ of the reduced spectrum of the training graphs with adjacency matrix \mathbf{A}_{gt} and 2) an adversarial loss on the generated adjacency matrix $\mathcal{A}(\tilde{\mathbf{\Phi}}, \tilde{\boldsymbol{\lambda}})$, *i.e.*,

$$L_{\text{rec}} = \text{BCE}(\mathbf{A}_{gt}, \mathcal{A}(\tilde{\mathbf{\Phi}}_{gt}, \tilde{\boldsymbol{\lambda}}_{gt})) \quad (13)$$

$$L_{\text{adv}} = \log(\mathcal{D}(\mathbf{A}_{gt})) + \log(1 - \mathcal{D}(\mathcal{A}(\tilde{\mathbf{\Phi}}, \tilde{\boldsymbol{\lambda}}))), \quad (14)$$

where BCE is the standard binary cross entropy loss and \mathcal{D} is a discriminator network composed of a sequence of PPGN layers followed by a global pooling for the final graph-level classification. Note that, unlike in SPECTRE (Martinkus

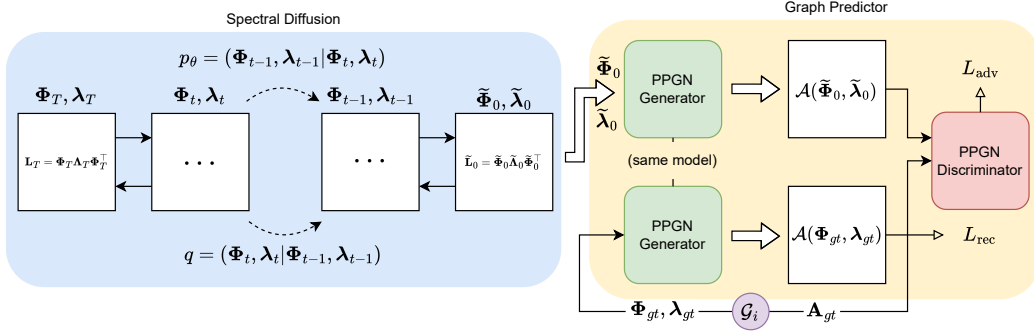


Figure 1: GRASP pipeline. During the spectral diffusion process (left) the neural network is trained to predict the denoising steps for the eigenvectors ϕ and eigenvalues λ of the graph Laplacian. The second stage of our method is the graph predictor (right), where we train a Provably Powerful Graph Network (PPGN) (Maron et al., 2019) (similar to what was done in SPECTRE (Martinkus et al., 2022)). Given the eigenvalues and eigenvectors generated, it predicts the adjacency matrix.

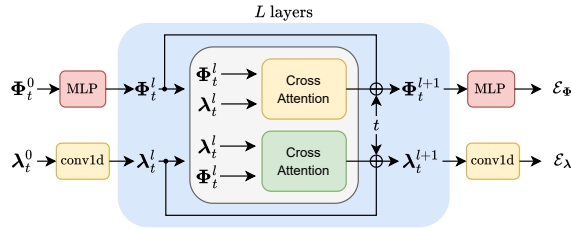


Figure 2: The score model takes as input the noisy eigenvector matrix and eigenvalues at time t and predicts the noise of the data to be used in the denoising step. The k node feature eigenvectors Φ_t^0 are projected through an MLP to a d dimensional space. The sequence of k eigenvalues is given as input to a 1D convolutional layer, which outputs d features for each eigenvalue. Both eigenvectors and eigenvalues go through a series of L layers composed of two multi-head cross-attention blocks, one updating the eigenvectors conditioned by the eigenvalues and one updating the eigenvalues conditioned on the eigenvectors. After each layer, we apply a residual block \oplus , which adds to the layer input the updated values scaled and shifted by time-dependent factors. Finally, Φ_t^L and λ_t^L are projected to a k dimensional space through an MLP and a 1D convolution.

et al., 2022), this refining step is not generative, meaning that the output is deterministic and depends solely on the input eigenvectors/values.

6. Experimental Evaluation

Datasets. We compare the performance of our model against that of state-of-the-art alternatives on both synthetic and real-world datasets. As commonly done in the literature, we use three synthetic datasets and two real-world datasets. The synthetic datasets we consider are (i) Community-small ($12 \leq |V| \leq 20$), (ii) Planar ($|V| = 64$), and (iii)

Stochastic Block Model (SBM) (2-5 communities and 20-40 nodes per community). The real-world datasets are both from the molecular domain, namely (i) Proteins (100-500 nodes) (Dobson & Doig, 2003) and (ii) QM9 (9 nodes) (Rudigkeit et al., 2012; Ramakrishnan et al., 2014). Detailed descriptions of all datasets can be found in Appendix A.

Statistics-Based Evaluation Metrics. We assess the ability of the models to generate graphs with structural characteristics close to those of the training graphs by following the methodology outlined in (Liao et al., 2019), which aims to address the difficulties of measuring likelihoods when evaluating autoregressive graph generative models reliant on orderings. In particular, we adopt the approach proposed by (You et al., 2018b) and (Li et al., 2018a) and used by many others (Krawczuk et al., 2020) as well. Our evaluation centers on contrasting the distributions of graph statistics between the generated and actual graphs.

Specifically, we consider the following key graph statistics: degree distribution (Deg.), clustering coefficient (Clus.), and the occurrence frequency of all 4-node orbits (Orb.). The deviation of these metrics between the generated graphs and the actual ones is measured using the maximum mean discrepancy (MMD) (You et al., 2018b). In its initial formulation, the computation of the MMD relied on the Earth Mover’s Distance (EMD) and as a result was very slow. For this reason, as suggested in (Liao et al., 2019), we use the total variational (TV) Gaussian kernel. This in turn significantly accelerates the evaluation process while maintaining consistency with EMD. In addition to assessing node degree, clustering coefficient, and orbit counts, we also extend our evaluation to include a spectral analysis (Spect.), following (Liao et al., 2019). This involves computing the eigenvalues of the normalized graph Laplacian, quantized to approximate a probability density. The spectral comparison offers insights into the global properties of the graphs, com-

plementing the local graph statistics emphasized by previous metrics.

Intrinsic-Quality-Based Evaluation Metrics. In addition to assessing the similarity between real and generated graphs, three key metrics are commonly used to directly evaluate the quality of the generated graphs: validity, uniqueness, and novelty (Samanta et al., 2020; Guo & Zhao, 2022). It is important to note that, in this work, these metrics are exclusively applied to real graphs.

The *validity* is determined by the ratio of valid molecules to all generated molecules. For molecule graphs, the validity in molecule generation represents the percentage of chemically valid molecules based on specific domain rules. We measure it using RDKit sanitization².

The *novelty* gauges the percentage of generated graphs that are not sub-graphs of the training set, and vice versa. It checks if the model has successfully learned to generalize to unseen graphs and it considers two graphs identical if they are isomorphic.

The *uniqueness* is defined as the ratio of unique samples to valid samples, measuring the level of variety during sampling. To calculate uniqueness, generated graphs that are sub-graph isomorphic to others are initially removed, and the remaining percentage represents uniqueness. For instance, if a model generates 100 identical graphs, the uniqueness is $1/100 = 1\%$.

The three metrics can be combined to evaluate the percentage of graphs that are valid (if applicable), unique, and novel.

Baselines. We evaluate the effectiveness of our model by comparing it against a number of well established graph generative models as well as some recently developed deep graph generative models. In particular, we consider GraphRNN (You et al., 2018b), GRAN (Liao et al., 2019), DiGress (Vignac et al., 2022), and SPECTRE (Martinkus et al., 2022). For the molecule generation task we also include GraphVAE (Simonovsky & Komodakis, 2018).

6.1. Evaluating the Generated Graphs

Synthetic Datasets The types of synthetic graphs we consider (planar, SBM, and community-small) are the same of (Martinkus et al., 2022). However, in order to achieve more robust results, we adopt a slightly different evaluation procedure compared to previous works. Specifically, we generated new test sets with identical characteristics but larger in size. We constructed a test set consisting of 200 graphs for planar and SBM, while for community-small, we generated a test set of 100 graphs. This in turn implies

²https://www.rdkit.org/docs/RDKit_Book.html

Table 1: Community-small Dataset. Comparison with other graph generative models using MMD metrics (the smaller the better).

	Community-Small			
	Deg. ↓	Clus. ↓	Spect. ↓	Orb. ↓
GraphRNN	0.02711	0.10725	0.05196	0.14682
GRAN	0.00135	<u>0.08427</u>	<u>0.02816</u>	<u>0.02013</u>
DiGress	0.00964	0.10351	0.05065	0.03721
SPECTRE	0.00786	0.10669	0.04597	0.02495
GRASP	<u>0.00160</u>	0.05900	0.01528	0.01426

Table 2: Planar dataset. Comparison with other graph generative models using MMD metrics (the smaller the better). We were unable to replicate the results reported for SPECTRE in (Martinkus et al., 2022) by using the code provided by the authors on GitHub.

	Planar Graphs			
	Deg. ↓	Clus. ↓	Spect. ↓	Orb. ↓
GraphRNN	0.00959	0.29855	0.03891	1.40225
GRAN	0.02020	0.29848	0.02480	0.19644
DiGress	0.00050	0.01783	0.00203	<u>0.01152</u>
SPECTRE*	0.29816	0.33862	0.13289	1.68168
GRASP	<u>0.00125</u>	0.18809	<u>0.00572</u>	0.00469

that we have also employed a greater number of generated graphs to compute the MMD measures, equivalent to the cardinality of the test sets.

The experimental results for community-small, SBM, and planar are shown in Table 1, Table 2, and Table 3, respectively. In these tables, we report the MMD metrics for the graph statistics, where the smaller the statistics, the better. The best performance is highlighted in bold, while the second-best value is underlined.

Overall, our model consistently achieves the best or second-best results across all datasets, with the exception of *Spect.* in SBM. In community-small, our model excels in all statistics except for the degree, where we rank as the second-best method. Similarly, in planar, our results closely align with the top-performing methods. Notably, SBM stands out as the only dataset where our performance is comparatively lower, as we do not rank among the top two performers across all statistics. Although not shown in the table, it is worth noting that our method achieves 100% uniqueness on both SBM and planar.

Real-world Datasets We also followed a different and more robust protocol to evaluate the generated graphs on

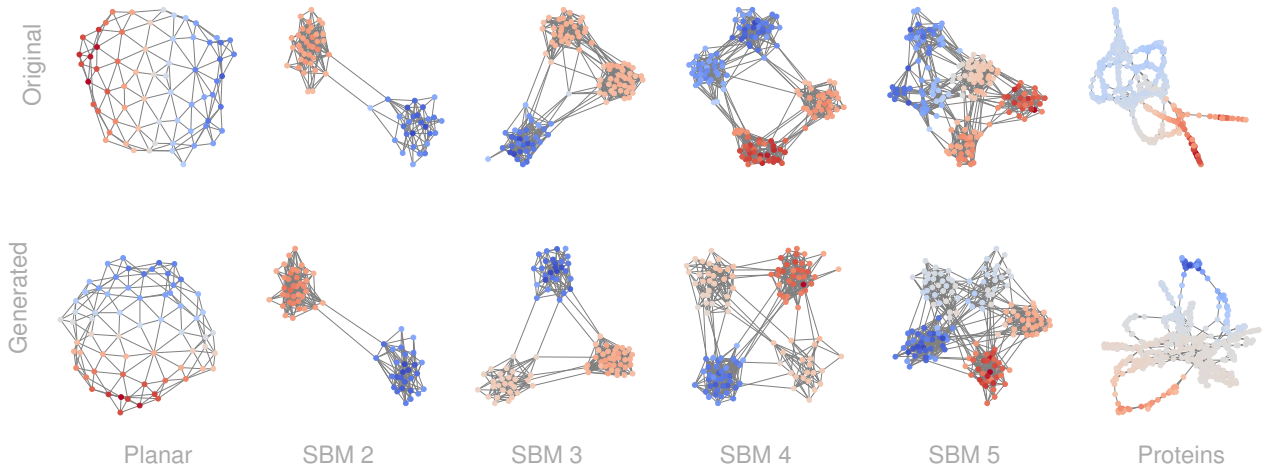


Figure 3: Visual comparison between training set graph samples and generated graph samples produced by GRASP. Each column represents a graph type (planar, stochastic block model with 2, 3, 4, and 5 communities, and proteins). Top row (Original): training set graphs. Bottom row (Generated): graph generated by GRASP.

Table 3: Stochastic Block Model dataset. Comparison with other graph generative models using MMD metrics (the smaller the better).

	Stochastic Block Model			
	Deg. ↓	Clus. ↓	Spect. ↓	Orb. ↓
GraphRNN	0.01784	0.01515	0.01040	0.03513
GRAN	0.01348	0.01488	<u>0.00342</u>	0.03516
DiGress	0.01656	0.02459	0.00644	0.13271
SPECTRE	<u>0.00444</u>	<u>0.01184</u>	0.00150	0.01399
GRASP	0.00055	0.01152	0.00454	<u>0.02890</u>

the Proteins dataset. Rather than utilizing a single subset of the dataset as a test set, we created 10 folds (equivalent for each method) thus enabling us to report the average of each metric (\pm standard deviation) over the 10 folds.

In the real-world graph datasets, it is interesting to observe how our method has unquestionably outperformed all other approaches, as indicated in Table 4 and Table 5.

Regarding the Proteins dataset, the metrics presented correspond to graph statistics. Across all measures, we rank as the best, except for the orbit metric where we still perform well. In the case of the QM9 dataset, we report metrics related to Intrinsic-Quality-Based criteria, where the higher the better. In Table 5, it is important to note that the last column is of particular interest as it summarizes all values, where we emerge as the top performers. We highlight that

for the DiGress method, we utilized their checkpoints to generate the graphs.

6.2. Graph Predictor Ablation

Given that the “Graph Predictor” is trained using a discriminative loss, one may think that it is this component that is doing all the “heavy lifting” of the graph generation task, while the “Spectral Diffusion” may be just producing noisy data.

To assess that this is not the case, we designed an experiment training our model to predict all the eigenvectors and eigenvalues on the community-small dataset. The small size of the graphs in this datasets allows us to generate all the eigenvectors Φ and eigenvalues λ and reconstruct the exact Laplacian $L = \Phi \Lambda \Phi^T$ and the (almost) binary adjacency matrix $A = D - L$. In table 6 we show three different configurations of our method: 1) in “Only Diffusion” we use the technique we just described, in which the graph is constructed directly from the generated Φ and λ without using the “Graph Predictor”; 2) in “Noise + Predictor” we give as input to the “Graph Predictor” noise drawn from a Gaussian distribution; 3) “Diff. + Prediction” is the full model which we use in all the other experiments. Reconstructing the graph directly from the Laplacian, in the case of the complete spectrum, leads to the best result while using random noise as input to the Predictor leads to significantly worse results. This in turn means that the actual generation is being performed by the “Spectral Diffusion” part of the network.

Table 4: Proteins dataset. Comparison with other graph generative models using MMD metrics (the smaller the better). Mean \pm and standard deviation are shown - measures calculated by averaging over 10 folds.

Proteins				
	Deg. \downarrow	Clus. \downarrow	Spect \downarrow	Orbit \downarrow
GraphRNN	0.00655 \pm 0.00106	0.16584 \pm 0.00883	0.01704 \pm 0.00094	0.81416 \pm 0.02733
GRAN	0.05688 \pm 0.00560	0.16218 \pm 0.00921	0.01459 \pm 0.00074	0.34298 \pm 0.03629
SPECTRE	<u>0.00823\pm0.00214</u>	<u>0.09881\pm0.00713</u>	<u>0.00661\pm0.00044</u>	0.03282\pm0.00390
GRASP	0.00145\pm0.00062	0.08072\pm0.00699	0.00257\pm0.00024	<u>0.12617\pm0.02354</u>

Table 5: QM9 dataset, molecule generation. Comparison with other graph generative models based on validity, uniqueness, and novelty metrics (the higher the better). Baseline results are taken from (Martinkus et al., 2022) and (Vignac et al., 2022).

QM9			
	Val. \uparrow	Val.& Uniq. \uparrow	Val.& Uniq.& Nov. \uparrow
GraphVAE	0.5570	0.4200	0.2610
DiGress	0.9900	0.9523	<u>0.3180</u>
SPECTRE	0.8730	0.3120	0.2910
GRASP	0.7430	0.5615	0.4531

Table 6: Ablation of the Graph Predictor network on the community-small dataset

	Deg. \downarrow	Clus. \downarrow	Spect. \downarrow	Orb. \downarrow
Only Diffusion	0.00134	0.05484	0.01574	0.00514
Noise + Predictor	0.04428	0.11129	0.05691	0.46051
Diff. + Predictor	0.00562	0.07887	0.02232	0.00942

6.3. Spectral conditioned generation

The spectrum of the Laplacian plays a relevant role in many applications, ranging from graph classification and mesh analysis (Bai et al., 2015; Hu et al., 2014) to reconstructing the underlying geometry of a triangulated 3D shape (Cosmo et al., 2019; Marin et al., 2021). Being able to generate a graph given a target spectrum is thus an important feature of a generative method.

We pose the graph generation conditioned on a sequence of eigenvalues as an inpainting problem (Lugmayr et al., 2022). The eigenvectors at time $t - 1$ are computed according to Eq. 11, while the eigenvalues are derived from the target ones through the forward diffusion process (Eq. 3):

Table 7: Spectral conditioning on the SBM dataset.

Generated communities:	2	3	4	5
Target $\tilde{\lambda}$ of 2 communities	0	74	19	5
Target $\tilde{\lambda}$ of 3 communities	0	12	86	0

$$\begin{aligned} \lambda_{t-1} &\sim \mathcal{N}(\sqrt{\bar{\alpha}_t}\lambda_0, (1 - \bar{\alpha}_t)\mathbf{I}) \\ \Phi_{t-1} &\sim \mathcal{N}(\Phi_{t-1}; \mu_\theta(\Phi_t, \lambda_t; t), \sigma_t^2\mathbf{I}) \end{aligned} \quad (15)$$

To validate the generation conditioned on the eigenvalues we generate graphs of the SBM data distribution by fixing the number of nodes as the average number of nodes of graphs containing 2 and 3 communities (70 nodes). We then generate 100 graphs conditioning with the spectrum of a graph with 2 communities and 100 graphs conditioning with the spectrum of 3 communities. The results reported in Table 7 show that spectral conditioning is indeed able to influence the properties of the generated graphs.

7. Conclusion

We have introduced GRASP, a diffusion-based generative model for graphs where the spectrum of the graph Laplacian is used to retain structural information while reducing the computational complexity. Our approach has a number of advantages, from the ability to directly generate eigenvectors and eigenvalues, to the possibility of naturally encapsulate node feature information as well as conditioning the generation on target spectral properties.

Acknowledgements

This project is partially supported by the PRIN 2022 project n. 2022AL45R2 (EYE-FLAI, CUP H53D2300350-0001). G.M. acknowledges financial support from project iNEST (Interconnected NordEst Innovation Ecosystem), funded by European Union Next - GenerationEU - National Recovery and Resilience Plan (NRRP) - MISSION 4 COMPONENT 2, INVESTMENT N. ECS00000043

– CUP N. H43C22000540006. In this regard, the manuscript reflects only the authors’ views and opinions, neither the European Union nor the European Commission can be considered responsible for them.

References

- Albert, R. and Barabási, A.-L. Statistical mechanics of complex networks. *Reviews of modern physics*, 74(1):47, 2002.
- Bai, L., Rossi, L., Torsello, A., and Hancock, E. R. A quantum jensen–shannon graph kernel for unattributed graphs. *Pattern Recognition*, 48(2):344–355, 2015.
- Cosmo, L., Panine, M., Rampini, A., Ovsjanikov, M., Bronstein, M. M., and Rodolà, E. Isospectralization, or how to hear shape, style, and correspondence. In *IEEE Conference on Computer Vision and Pattern Recognition, CVPR 2019, Long Beach, CA, USA, June 16-20, 2019*, pp. 7529–7538. Computer Vision Foundation / IEEE, 2019. doi: 10.1109/CVPR.2019.00771.
- De Cao, N. and Kipf, T. Molgan: An implicit generative model for small molecular graphs. *arXiv preprint arXiv:1805.11973*, 2018.
- Dobson, P. D. and Doig, A. J. Distinguishing enzyme structures from non-enzymes without alignments. *Journal of molecular biology*, 330(4):771–783, 2003.
- Erdős, P., Rényi, A., et al. On the evolution of random graphs. *Publ. math. inst. hung. acad. sci.*, 5(1):17–60, 1960.
- Faloutsos, C. Graph mining: Laws, generators and tools. *Lecture Notes in Computer Science*, 5012:1, 2008.
- Feller, W. On the theory of stochastic processes, with particular reference to applications. In *Proceedings of the [First] Berkeley Symposium on Mathematical Statistics and Probability*, pp. 403–432, 1949.
- Gómez-Bombarelli, R., Wei, J. N., Duvenaud, D., Hernández-Lobato, J. M., Sánchez-Lengeling, B., Sheberla, D., Aguilera-Iparraguirre, J., Hirzel, T. D., Adams, R. P., and Aspuru-Guzik, A. Automatic chemical design using a data-driven continuous representation of molecules. *ACS central science*, 4(2):268–276, 2018.
- Goodfellow, I., Pouget-Abadie, J., Mirza, M., Xu, B., Warde-Farley, D., Ozair, S., Courville, A., and Bengio, Y. Generative adversarial nets. *Advances in neural information processing systems*, 27, 2014.
- Grover, A., Zweig, A., and Ermon, S. Graphite: Iterative generative modeling of graphs. In *International conference on machine learning*, pp. 2434–2444. PMLR, 2019.
- Guo, X. and Zhao, L. A systematic survey on deep generative models for graph generation. *IEEE Transactions on Pattern Analysis and Machine Intelligence*, 45(5):5370–5390, 2022.
- Haefeli, K. K., Martinkus, K., Perraudin, N., and Wattenhofer, R. Diffusion models for graphs benefit from discrete state spaces. *arXiv preprint arXiv:2210.01549*, 2022.
- Ho, J., Jain, A., and Abbeel, P. Denoising diffusion probabilistic models. *Advances in neural information processing systems*, 33:6840–6851, 2020.
- Hu, N., Rustamov, R. M., and Guibas, L. Stable and informative spectral signatures for graph matching. In *Proceedings of the IEEE conference on computer vision and pattern recognition*, pp. 2305–2312, 2014.
- Huang, H., Sun, L., Du, B., Fu, Y., and Lv, W. Graphgdp: Generative diffusion processes for permutation invariant graph generation. In *2022 IEEE International Conference on Data Mining (ICDM)*, pp. 201–210. IEEE, 2022.
- Jo, J., Lee, S., and Hwang, S. J. Score-based generative modeling of graphs via the system of stochastic differential equations. In *International Conference on Machine Learning*, pp. 10362–10383. PMLR, 2022.
- Kingma, D. P. and Welling, M. Auto-encoding variational bayes. *arXiv preprint arXiv:1312.6114*, 2013.
- Krawczuk, I., Abranches, P., Loukas, A., and Cevher, V. Ggan: A geometric graph generative adversarial network. 2020.
- Leskovec, J. and Faloutsos, C. Scalable modeling of real graphs using kronecker multiplication. In *Proceedings of the 24th international conference on Machine learning*, pp. 497–504, 2007.
- Leskovec, J., Chakrabarti, D., Kleinberg, J., Faloutsos, C., and Ghahramani, Z. Kronecker graphs: an approach to modeling networks. *Journal of Machine Learning Research*, 11(2), 2010.
- Li, Y., Vinyals, O., Dyer, C., Pascanu, R., and Battaglia, P. Learning deep generative models of graphs. *arXiv preprint arXiv:1803.03324*, 2018a.
- Li, Y., Zhang, L., and Liu, Z. Multi-objective de novo drug design with conditional graph generative model. *Journal of cheminformatics*, 10:1–24, 2018b.
- Liao, R., Li, Y., Song, Y., Wang, S., Hamilton, W., Duvenaud, D. K., Urtasun, R., and Zemel, R. Efficient graph generation with graph recurrent attention networks. *Advances in neural information processing systems*, 32, 2019.

- Lugmayr, A., Danelljan, M., Romero, A., Yu, F., Timofte, R., and Van Gool, L. Repaint: Inpainting using denoising diffusion probabilistic models. 2022.
- Luo, T., Mo, Z., and Pan, S. J. Fast graph generation via spectral diffusion. *IEEE Transactions on Pattern Analysis and Machine Intelligence*, 2023.
- Luo, Y., Yan, K., and Ji, S. Graphdf: A discrete flow model for molecular graph generation. In *International Conference on Machine Learning*, pp. 7192–7203. PMLR, 2021.
- Marin, R., Rampini, A., Castellani, U., Rodolà, E., Ovsjanikov, M., and Melzi, S. Spectral shape recovery and analysis via data-driven connections. *Int. J. Comput. Vision*, 129(10):2745–2760, oct 2021. ISSN 0920-5691. doi: 10.1007/s11263-021-01492-6.
- Maron, H., Ben-Hamu, H., Serviansky, H., and Lipman, Y. Provably powerful graph networks. In Wallach, H., Larochelle, H., Beygelzimer, A., d'Alché-Buc, F., Fox, E., and Garnett, R. (eds.), *Advances in Neural Information Processing Systems*, volume 32. Curran Associates, Inc., 2019. URL https://proceedings.neurips.cc/paper_files/paper/2019/file/bb04af0f7ecaee4aae62035497da1387-Paper.pdf.
- Martinkus, K., Loukas, A., Perraudin, N., and Wattenhofer, R. Spectre: Spectral conditioning helps to overcome the expressivity limits of one-shot graph generators. In *International Conference on Machine Learning*, pp. 15159–15179. PMLR, 2022.
- Niu, C., Song, Y., Song, J., Zhao, S., Grover, A., and Ermon, S. Permutation invariant graph generation via score-based generative modeling. In *International Conference on Artificial Intelligence and Statistics*, pp. 4474–4484. PMLR, 2020.
- Popova, M., Shvets, M., Oliva, J., and Isayev, O. Molecular-rnn: Generating realistic molecular graphs with optimized properties. *arXiv preprint arXiv:1905.13372*, 2019.
- Ramakrishnan, R., Dral, P. O., Rupp, M., and Von Lilienfeld, O. A. Quantum chemistry structures and properties of 134 kilo molecules. *Scientific data*, 1(1):1–7, 2014.
- Ruddigkeit, L., Van Deursen, R., Blum, L. C., and Reymond, J.-L. Enumeration of 166 billion organic small molecules in the chemical universe database gdb-17. *Journal of chemical information and modeling*, 52(11):2864–2875, 2012.
- Samanta, B., De, A., Jana, G., Gómez, V., Chattaraj, P., Ganguly, N., and Gomez-Rodriguez, M. Nevae: A deep generative model for molecular graphs. *Journal of machine learning research*, 21(114):1–33, 2020.
- Shi, C., Xu, M., Zhu, Z., Zhang, W., Zhang, M., and Tang, J. Graphaf: a flow-based autoregressive model for molecular graph generation. *arXiv preprint arXiv:2001.09382*, 2020.
- Simonovsky, M. and Komodakis, N. Graphvae: Towards generation of small graphs using variational autoencoders. In *Artificial Neural Networks and Machine Learning—ICANN 2018: 27th International Conference on Artificial Neural Networks, Rhodes, Greece, October 4-7, 2018, Proceedings, Part I 27*, pp. 412–422. Springer, 2018.
- Sohl-Dickstein, J., Weiss, E., Maheswaranathan, N., and Ganguli, S. Deep unsupervised learning using nonequilibrium thermodynamics. In *International conference on machine learning*, pp. 2256–2265. PMLR, 2015.
- Song, Y. and Ermon, S. Generative modeling by estimating gradients of the data distribution. *Advances in neural information processing systems*, 32, 2019.
- Vaswani, A., Shazeer, N., Parmar, N., Uszkoreit, J., Jones, L., Gomez, A. N., Kaiser, L. u., and Polosukhin, I. Attention is all you need. In Guyon, I., Luxburg, U. V., Bengio, S., Wallach, H., Fergus, R., Vishwanathan, S., and Garnett, R. (eds.), *Advances in Neural Information Processing Systems*, volume 30. Curran Associates, Inc., 2017. URL https://proceedings.neurips.cc/paper_files/paper/2017/file/3f5ee243547dee91fbd053c1c4a845aa-Paper.pdf.
- Vignac, C., Krawczuk, I., Siraudin, A., Wang, B., Cevher, V., and Frossard, P. Digress: Discrete denoising diffusion for graph generation. *arXiv preprint arXiv:2209.14734*, 2022.
- Watts, D. J. and Strogatz, S. H. Collective dynamics of ‘small-world’ networks. *nature*, 393(6684):440–442, 1998.
- Yoon, M., Wu, Y., Palowitch, J., Perozzi, B., and Salakhutdinov, R. Graph generative model for benchmarking graph neural networks. 2023.
- You, J., Liu, B., Ying, Z., Pande, V., and Leskovec, J. Graph convolutional policy network for goal-directed molecular graph generation. *Advances in neural information processing systems*, 31, 2018a.
- You, J., Ying, R., Ren, X., Hamilton, W., and Leskovec, J. Graphrnn: Generating realistic graphs with deep autoregressive models. In *International conference on machine learning*, pp. 5708–5717. PMLR, 2018b.
- Zaremba, W., Sutskever, I., and Vinyals, O. Recurrent neural network regularization. *arXiv preprint arXiv:1409.2329*, 2014.

A. Datasets.

For evaluation, we leverage these five commonly used datasets.

Community-small: A synthetic dataset consisting of 100 random community graphs, with [12, 20] nodes.

Stochastic Block Model (SBM): A synthetic dataset from (Martinkus et al., 2022) comprising 200 Stochastic Block Model graphs, each with a random selection of 2 to 5 communities and 20 to 40 nodes within each community. The probability of edges between communities is set at 0.3, while the probability of edges within communities is set at 0.05.

Planar: A synthetic dataset from (Martinkus et al., 2022) of 200 planar graphs, each containing 64 nodes. Graphs are created through the application of Delaunay triangulation to a randomly and uniformly placed set of points.

QM9 (Ramakrishnan et al., 2014; Ruddigkeit et al., 2012): This real-world dataset comprises 134k organic molecules with a maximum of 9 heavy atoms (carbon, oxygen, nitrogen, and fluorine). By following (Simonovsky & Komodakis, 2018) we allocate 10k molecules for validation, 10k for testing, and the rest for training.

Proteins (Dobson & Doig, 2003): The dataset encompasses 918 protein graphs, each ranging from 100 to 500 nodes. In this representation, each protein is depicted as a graph, with nodes corresponding to amino acids. Nodes are connected by an edge if they are within a distance of less than 6 Angstroms from each other.

B. Number of Eigenvectors

To assess the importance of the number of eigenvectors and the part of the spectra which is more relevant, we performed an experiment on community-small training our model with an increasing number of eigenvectors, either keeping the smallest eigenvalues (Smallest) or the largest (Largest).

The results in Table 8 show how keeping more eigenvalues helps the reconstruction, and how the largest eigenvalues are generally more informative. In our experiments, we used the 32 larger eigenvectors/values for all the datasets, except for community-small in which we used 8 eigenvectors.

C. Implementation Details

For the training of the diffusion model, we split each dataset into 90% train and 10% test, and we train the Spectral Diffusion on the whole dataset for 100k epochs, using early stopping on the reconstruction loss. We performed a grid search on the number of layers between 6, 9 and 12, and selected the best model according to the degree metric computed

Table 8: Number of eigenvectors

		Degree			
# eigenvectors:		4	8	12	16
	Smallest	0.0498	0.0580	0.0048	0.0023
	Largest	0.0035	0.0048	0.0042	0.0031
		Cluster			
# eigenvectors:		4	8	12	16
	Smallest	0.2420	0.1725	0.1633	0.1603
	Largest	0.2687	0.1400	0.1170	0.1007
		Spectral			
# eigenvectors:		4	8	12	16
	Smallest	0.0528	0.0486	0.0479	0.0567
	Largest	0.0571	0.0435	0.0327	0.0465

from the graphs reconstructed directly from the eigenvectors/values and the graphs of the training set. The sampling has been done using DDIM with 100 steps. Moreover, we generate each sample 4 times and keep the one with the lower deviation from orthogonality.

For the training of the Graph Predictor, we used the same splits of the Spectral Diffusion, and trained for 100k epochs. We performed early stopping by comparing the degree distribution of the generated graphs with the training graphs. We used 6 PPGN layers and 3 PPGN layers for the Graph Predictor and the discriminator network respectively, except for QM9 in which also the Graph Predictor is composed of three layers. For QM9, we let the Graph Predictor to generate also edge features, similarly to (Martinkus et al., 2022).

As mentioned in Appendix B, in all our experiments we trained our model using the largest 32 eigenvectors/values, except for community-small, which uses just 8 eigenvectors/values.